

# Leptoquark Signals via $\nu$ interactions at Neutrino Factories

Poonam Mehta <sup>a, 1</sup>, Sukanta Dutta <sup>b, 2</sup> and Ashok Goyal <sup>a, c, 3</sup>

<sup>a</sup>*Department of Physics & Astrophysics, University of Delhi, Delhi 110 007, India*

<sup>b</sup>*Physics Department, S.G.T.B. Khalsa College, University of Delhi, Delhi 110 007, India*

<sup>c</sup>*Inter University Center for Astronomy & Astrophysics, Ganeshkhind, Pune 411 007, India*

## Abstract

The accurate prediction of neutrino beam produced in muon decays and the absence of opposite helicity contamination for a particular neutrino flavour makes a future neutrino factory (NF) based on a muon storage ring (MSR), the ideal place to look for the lepton flavour violating (LFV) effects. In this letter, we address the contribution of mediating LFV leptoquarks (LQ) in  $\nu(\bar{\nu}) - N$  interactions leading to production of  $\tau$ 's and wrong sign  $\mu$ 's at MSR and investigate the region where LQ interactions are significant in the near-site and short baseline experiments.

Keywords : Leptoquark, Muon storage ring, Lepton Flavour Violation, Neutrino.

## 1 Introduction

Recent results from Super Kamiokande and other experiments [1] strongly suggest  $\nu_\mu - \nu_\tau$  oscillation as the dominant oscillation mode, in order to explain the atmospheric  $\nu_\mu$  deficit. Similarly, the results for solar neutrino problem point towards  $\nu_e - \nu_\mu$  oscillation as the favoured solution [2]. In fact, the prime goal of next generation neutrino physics experimental studies ( for eg. NF based on MSR ) is to explore the physics beyond SM to unfold the mystery of the neutrino mass hierarchy and confirm the nature of neutrino flavour conversion [3]. At MSR with a  $\mu^-$  ( $\mu^+$ ) beam, roughly  $\simeq 10^{20}$  muons are allowed to decay per year giving rise to nearly equal number of  $\nu_\mu$  ( $\bar{\nu}_\mu$ ) and  $\bar{\nu}_e$  ( $\nu_e$ ). These  $\nu$  ( $\bar{\nu}$ )'s at the detector, may or may not have changed their flavour due to oscillation of neutrino mass eigenstates, which on interaction with matter produce associated charged leptons [4]. However, there can be effective LFV interactions motivated from new physics which may give rise to charged leptons in the final state as expected through  $\nu(\bar{\nu})$ -oscillations [5].

In this backdrop, it is worthwhile to study the production of  $\tau$  and wrong sign  $\mu$  via LQ as mediators which occur naturally in Grand Unified Theories, Superstring inspired  $E_6$  models and in Technicolor models [6]. There have been numerous phenomenological studies to put constraints on LQ from low energy flavour changing neutral current (FCNC) processes which are generated by both the scalar and vector LQ interactions, since there is no reason why the quark-lepton couplings with LQ have to be simultaneously diagonal in quark and lepton mass matrices. Direct experimental searches for leptoquarks have also been carried out

---

<sup>1</sup>E-mail address: pm@ducos.ernet.in, pmehta@physics.du.ac.in

<sup>2</sup>E-mail address: Sukanta.Dutta@cern.ch

<sup>3</sup>E-mail address: agoyal@ducos.ernet.in, goyal@iucaa.ernet.in

at the e p collider and bounds obtained [7, 8]. In this letter, we compute and analyse the contribution of mediating LFV LQ in  $\nu(\bar{\nu})$ - $N$  charged current (CC) interactions, including constraints obtained from low energy phenomenology.

The most general expression for the event rate per kilo Ton (kT) of the target per year for any charged lepton flavour  $l_k$ , obtained via CC interaction of  $\nu_j$  beam<sup>1</sup> produced as a result of oscillation from an initial  $\nu_i$  beam can be written as :

$$\mathcal{N}_{l_k^-, l_k^+} = \mathcal{N}_n \int \frac{d^2 \sigma^{\nu, \bar{\nu}} \left( \nu_j(\bar{\nu}_j) q \longrightarrow l_k^-(l_k^+) q' \right)}{dx dy} \left[ \frac{dN_{\nu, \bar{\nu}}}{dE_{\nu_i, \bar{\nu}_i}} \right] \mathcal{P}_{osc}(\nu_i(\bar{\nu}_i) \longrightarrow \nu_j(\bar{\nu}_j)) dE_{\nu_i(\bar{\nu}_i)} q(x) dx dy \quad (1)$$

where,  $\mathcal{N}_n$  is the number of nucleons present kT of the target material, x and y are the Bjorken scaling variables, q and q' are the quarks in the initial and final states, respectively and  $\mathcal{P}_{osc}$  is the oscillation probability. The differential parton level cross-section  $\frac{d^2 \sigma^{\nu, \bar{\nu}}}{dx dy}$  is  $\left[ \frac{|\mathcal{M}(x, y)|^2}{32\pi \hat{s}} \right] \left[ 2\lambda^{-1/2}(1, 0, \frac{m_l^2}{\hat{s}}) \right]$  where,  $\hat{s}$  is the parton level CM energy,  $m_l$  is the mass of the final-state lepton and  $\lambda^{1/2}(x, y, z) = x^2 + y^2 + z^2 - 2xy - 2xz - 2yz$  is the Michael parameter and  $\left[ \frac{dN_{\nu, \bar{\nu}}}{dE_{\nu_i, \bar{\nu}_i}} \right]$  is the differential  $\nu$  ( $\bar{\nu}$ ) flux. For the two flavour oscillation scenario<sup>2</sup>, the probability  $\mathcal{P}_{osc}(\nu_i \rightarrow \nu_j)$  is  $\sin^2 2\theta_m \sin^2 \left[ 1.27 \Delta m^2 [eV^2] \frac{L[km]}{E_\nu [GeV]} \right]$ , where,  $L$  is the baseline length,  $E_\nu$  is the neutrino energy,  $\Delta m^2$  is the mass-squared difference between the corresponding physical states, and  $\theta_m$  is mixing angle between flavours. Here  $q(x)$  is the quark distribution function. The general characteristics of  $\tau$  and wrong sign  $\mu$  production in the oscillation scenario (OS), for example are given by Dutta *et al.* [4].

The effective Lagrangian with the most general dimensionless,  $SU(3)_c X SU(2)_L X U(1)_Y$  invariant couplings of *scalar* and *vector* LQ satisfying baryon ( $B$ ) and lepton number ( $L$ ) conservation (suppressing colour, weak isospin and generation (flavour) indices ) is given [9] by:

$$\begin{aligned} \mathcal{L} &= \mathcal{L}_{|F|=2} + \mathcal{L}_{|F|=0} \quad \text{where} \\ \mathcal{L}_{|F|=2} &= [g_{1L} \bar{q}_L^c i \tau_2 l_L + g_{1R} \bar{u}_R^c e_R] S_1 + \tilde{g}_{1R} \bar{d}_R^c e_R \tilde{S}_1 + g_{3L} \bar{q}_L^c i \tau_2 \vec{\tau} l_L \vec{S}_3 \\ &+ [g_{2L} \bar{d}_R^c \gamma^\mu l_L + g_{2R} \bar{q}_L^c \gamma^\mu e_R] V_{2\mu} + \tilde{g}_{2L} \bar{u}_R^c \gamma^\mu l_L \tilde{V}_{2\mu} + \text{c.c.}, \\ \mathcal{L}_{|F|=0} &= [h_{2L} \bar{u}_R l_L + h_{2R} \bar{q}_L i \tau_2 e_R] R_2 + \tilde{h}_{2L} \bar{d}_R l_L \tilde{R}_2 + \tilde{h}_{1R} \bar{u}_R \gamma^\mu e_R \tilde{U}_{1\mu} \\ &+ [h_{1L} \bar{q}_L \gamma^\mu l_L + h_{1R} \bar{d}_R \gamma^\mu e_R] U_{1\mu} + h_{3L} \bar{q}_L \vec{\tau} \gamma^\mu l_L U_{3\mu} + \text{c.c.} \end{aligned} \quad (2)$$

where  $q_L, l_L$  are the left-handed quarks and lepton doublets and  $e_R, d_R, u_R$  are the right-handed charged leptons, down- and up-quark singlets respectively. The Scalar (i.e.  $S_1, \tilde{S}_1, S_3$ ) and Vector (i.e.  $V_2, \tilde{V}_2$ ) LQ carry fermion number  $F = 3B + L = -2$ , while the Scalar (i.e.  $R_2, \tilde{R}_2$ ) and Vector (i.e.  $U_1, \tilde{U}_1, U_3$ ) LQ have  $F = 0$ . Using this Lagrangian we discuss below the production of  $\tau$ 's and wrong sign  $\mu$ 's along with the standard Mass-Mixing solution of neutrino oscillation case.

## 2 Tau Appearance at a NF

We consider the production of  $\tau^-$  from unoscillated  $\nu_\mu$  (obtained from  $\mu^-$  decay) through LFV interactions with nucleon via u-channel processes for  $|F| = 0$  case (figure 1(a)) and s-

<sup>1</sup>  $k = j$  for the SM Lepton Flavour Conserving situation

<sup>2</sup> For the present case, it is sufficient to illustrate the main ideas by considering only the two flavour oscillations in vacuum.

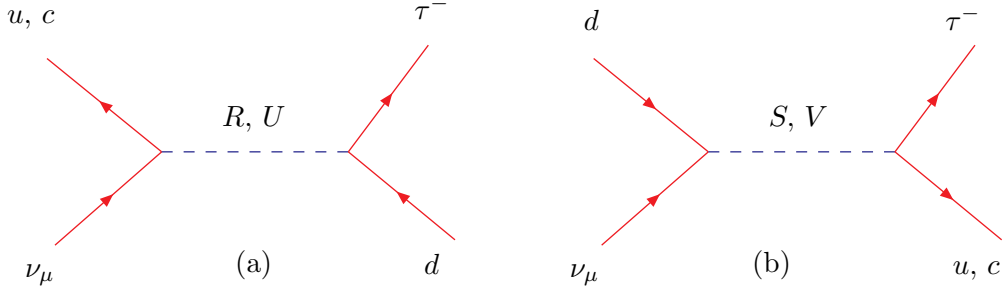


Figure 1:  $\tau^-$  from scalar  $\mathcal{E}^3$  vector LQ: (a)  $u$ -channel process corresponding to  $|F|=0$  LQ and (b)  $s$ -channel process corresponding to  $|F|=2$  LQ.

channel processes for  $|F| = 2$  case (figure 1(b)) LQ unlike OS where  $\tau^-$  are produced through interaction of  $\nu_\tau$  (oscillated from  $\nu_\mu$  with  $\Delta m^2 = 0.0023 \text{ eV}^2$  and  $\sin^2(2\theta_m) = 1.0$ ) with the nucleon. There are four processes contributing to  $\tau^-$  production in the  $u$ -channel (figure 1(a)), one mediated by the charge =  $2/3$ , scalar LQ ( $R_2$ ) with  $T_3 = -1/2$  and three by the vector LQ ( $U_{1\mu}, U_{1\mu}, U_{3\mu}$ ) with  $T_3 = 0$  each<sup>3</sup>, where  $T_3$  is the weak isospin. The matrix element squared for all the  $u$ -channel processes is

$$\begin{aligned}
 \left| \mathcal{M}_{LQ}^{u\text{-chann}}(\nu_\mu d \longrightarrow \tau^- u) \right|^2 &= \left[ \hat{u}(\hat{u} - m_\tau^2) \right] \left[ \frac{|h_{2L} h_{2R}|^2}{(\hat{u} - M_{R_2^a}^2)^2} \right] + \left[ 4\hat{s}(\hat{s} - m_\tau^2) \right] \left[ \frac{|h_{1L}|^4}{(\hat{u} - M_{U_{1\mu}}^2)^2} \right] \\
 &+ \frac{|h_{3L}|^4}{(\hat{u} - M_{U_{3\mu}}^2)^2} - 2 \frac{|h_{1L} h_{3L}|^2}{(\hat{u} - M_{U_{1\mu}}^2)(\hat{u} - M_{U_{3\mu}}^2)} + \left[ 4\hat{t}(\hat{t} - m_\tau^2) \right] \left[ \frac{|h_{1L} h_{1R}|^2}{(\hat{u} - M_{U_{1\mu}}^2)^2} \right] \quad (3)
 \end{aligned}$$

where, the Mandelstam variables at the parton level are given by  $\hat{s} = (p_{\nu_\mu} + p_d)^2$ ,  $\hat{t} = (p_{\nu_\mu} - p_{\tau^-})^2$  and  $\hat{u} = (p_{\nu_\mu} - p_{u,c})^2$ , with  $p_i$  denoting the four momentum of the  $i^{\text{th}}$  particle. In the  $s$ -channel, three processes are mediated by charge =  $-1/3$ , scalar LQ ( $S_1, S_1, S_3$ ) with  $T_3 = 0$ , while the fourth one is mediated by a vector LQ ( $V_2$ ) with  $T_3 = -1/2$  (figure 1(b))<sup>4</sup>. The matrix element squared for  $s$ -channel processes is

$$\begin{aligned}
 \left| \mathcal{M}_{LQ}^{s\text{-chann}}(\nu_\mu d \longrightarrow \tau^- u) \right|^2 &= \left[ \hat{s}(\hat{s} - m_\tau^2) \right] \left[ \frac{|g_{1L}|^4}{(\hat{s} - M_{S_1}^2)^2} + \frac{|g_{1L} g_{1R}|^2}{(\hat{s} - M_{S_1}^2)^2} + \frac{|g_{3L}|^4}{(\hat{s} - M_{S_3^a}^2)^2} \right. \\
 &\left. - 2 \frac{|g_{1L} g_{3L}|^2}{(\hat{s} - M_{S_1}^2)(\hat{s} - M_{S_3^a}^2)} \right] + \left[ 4\hat{t}(\hat{t} - m_\tau^2) \right] \left[ \frac{|g_{2L} g_{2R}|^2}{(\hat{s} - M_{V_{2\mu}}^2)^2} \right] \quad (4)
 \end{aligned}$$

In order to demonstrate the behaviour of the  $\tau$  production rate, we consider the contribution from LQ carrying different fermion numbers separately, which implies that *either* the  $h$ 's *or* the  $g$ 's (contributing to a given process) are non-zero at a time. For simplicity, we have taken the masses of scalar and vector LQ and couplings  $h$ 's ( $g$ 's) for  $|F| = 0$  ( $|F| = 2$ ) to be equal. We have used CTEQ4LQ parton distribution functions [10] to compute the event rates. To study the variation of  $\tau$  events w.r.t  $E_\mu$  and baseline length  $L$ , we have plotted the events for two different LQ masses 250 GeV & 500 GeV respectively using the product of couplings to be equal to  $\alpha_{em}$ . It should also be noted that since there are no strong bounds on the LQ

<sup>3</sup>In our notation,  $R_2^a$  denotes  $R_2$  with  $T_3 = -1/2$  and  $U_{3\mu}^a$  implies  $U_{3\mu}$  with  $T_3 = 0$ .

<sup>4</sup>In our notation,  $S_3^a$  denotes  $S_3$  with  $T_3 = 0$  and  $V_{2\mu}^a$  implies  $V_{2\mu}$  with  $T_3 = -1/2$ .

interacting with a charm quark and a  $\tau^-$  lepton existing in the literature, the cross-section for  $c\tau^-$  production in the  $\nu_\mu N$  DIS is governed by the flavour violating couplings between the second and third generation, which are not restricted by the bounds from the rare decays. The problem of charm detection and elimination of possible backgrounds however, needs to be tackled before the large available area in the parameter space can be explored. In figure

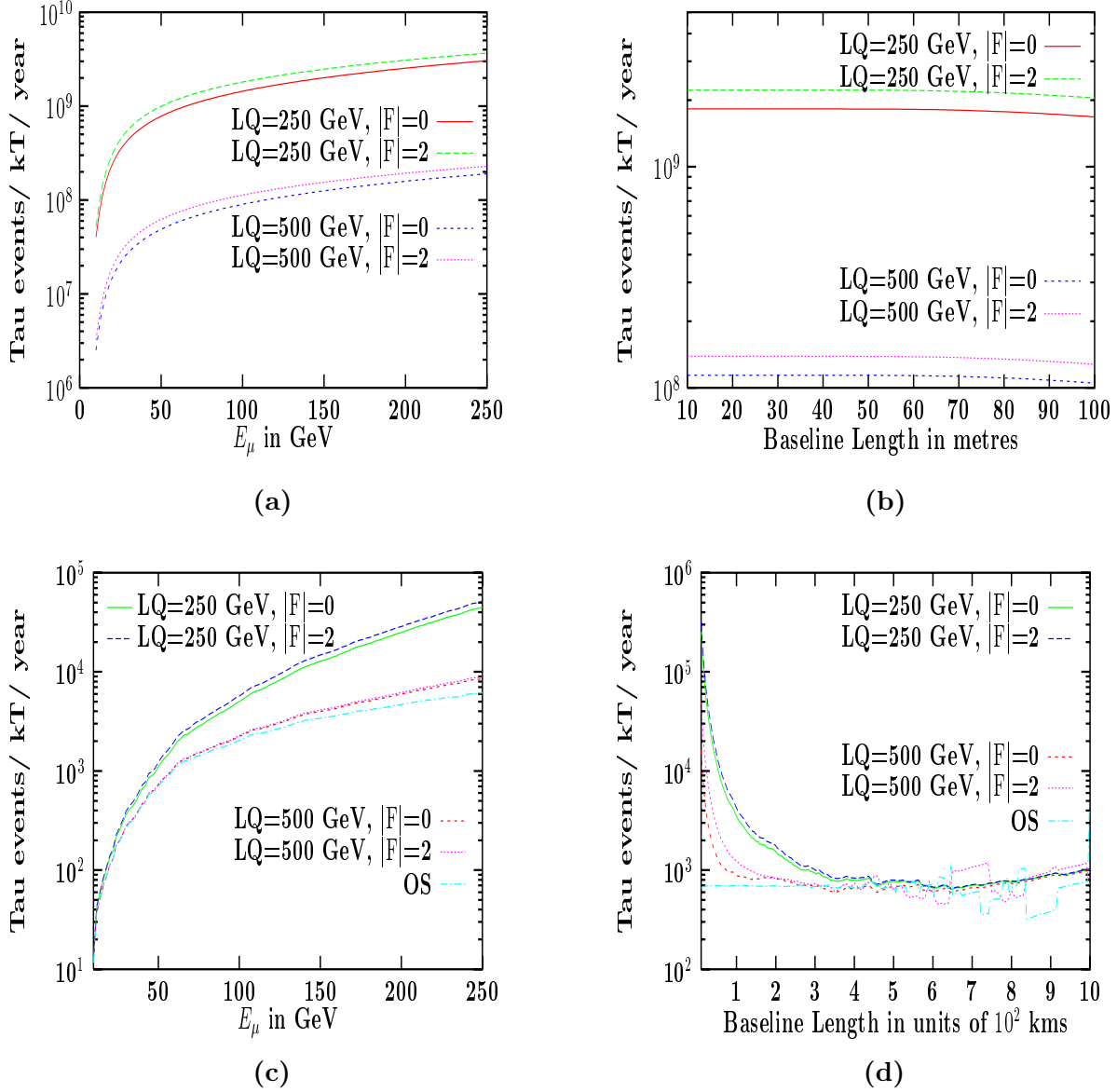


Figure 2: Variation  $\tau$ -events ( from osc. and LQ ) for a 1kT detector, LQ mass 250 & 500 GeV and product of LQ couplings = 0.089 with : (a) muon beam energy for a baseline length 40 meters and sample detector area 0.025 m<sup>2</sup>, (b) baseline length for muon beam energy 50 GeV and detector area 0.025 m<sup>2</sup>, (c) muon beam energy for a baseline length 250 kms and sample detector area 100 m<sup>2</sup>, (d) baseline length for muon beam energy 50 GeV and detector area 100 m<sup>2</sup>.

2(a), we plot the net contribution ( from LQ and oscillation ) to tau events for a near-site experimental set-up w.r.t  $E_\mu$ . We have considered a detector with a sample area of .025 m<sup>2</sup> [11] and placed at 40 mts from the storage ring. It is worthwhile to mention that the contribution is predominantly from LQ as the oscillation is suppressed at such baseline length. We

give similar curves in figure 2(c) with the detector placed at a baseline length of 250  $kms$  ( K2K Proposal, *from KEK to Kamioka* ) and sample detector area of 100  $m^2$  [11]. Here the contribution of LQ is comparable to that of the oscillation. Figure 2(b) shows the variation of events w.r.t. the baseline length, 1  $m$  to 100  $m$  (appropriate for near-site experiment) for  $E_\mu$  fixed at 50  $GeV$ . The graph clearly shows the independence of the tau events with baseline length in this range, while in figure 2(d) the behaviour of tau event rate is markedly different for short and medium baselines (1 – 1000  $kms$ ). Here, the LQ event rate falls off as  $1/L^2$  to zero and hence the combined event rate for  $\tau$  essentially merges with that due to oscillation alone.

The background for the signal of  $\tau$  and the ways to eliminate them have been already discussed in detail in the existing literature ( see for example, reference [12] ) and it is found out that the missing- $p_T$  and isolation cuts taken together can remove the entire set of backgrounds due to charmed particle production, from unoscillated CC events and from the neutral current background. Recently, there have been theories that propose the existence of an extra neutral boson in many extensions of SM which lead to  $\nu_\mu$  associated charm production [13], which also acts as a source of background and need to be eliminated as far as detection of  $\tau$  events are concerned. The  $\tau$ -detection efficiency factor of 30% [5, 11, 12] taken in the present calculation, adequately accounts for all the selection cuts ( including the cuts for missing  $p_T$ , isolation cut and the branching ratio ) required to eliminate the backgrounds.

**Sensitivity Limits :** An estimate of the sensitivity limits on product of couplings and LQ masses can be based on the total number of events. Here we determine the range of LQ masses and product of LFV couplings, for which the number of signal events is equal to two and five times the square root of the OS events. Accepting this requirement of  $2\sigma$  and  $5\sigma$  effect as a sensible discovery criterion, we plot the corresponding contours in figure 3 for baseline length=40 m. Thus, non compliance of these estimate with experimental observation would mean that the lower region enclosed by the curve are ruled out at  $2\sigma$  and  $5\sigma$  level, respectively.

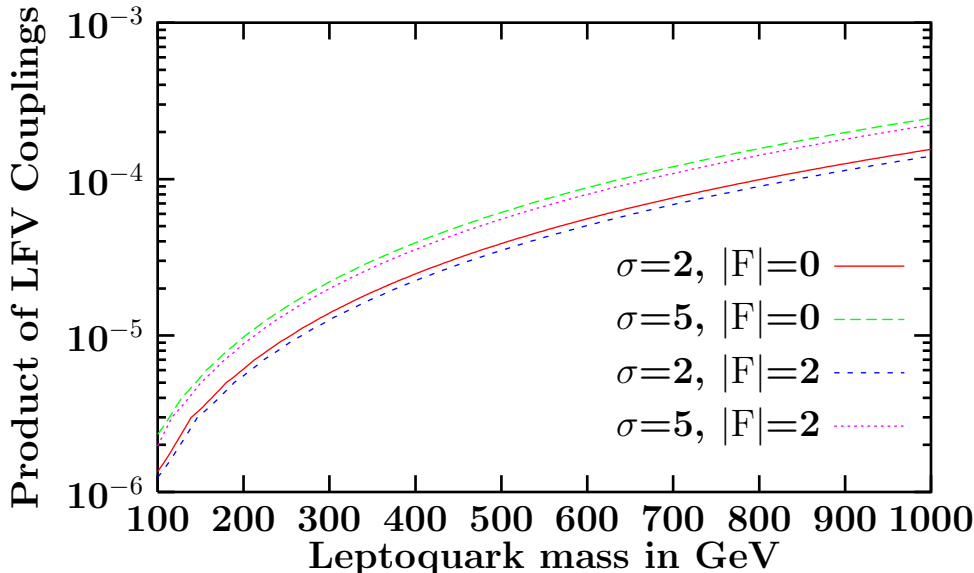


Figure 3: *Contours for  $2\sigma$  and  $5\sigma$  effect for  $E_\mu=50 GeV$ , baseline length=40 meters and sample detector of area 2500  $cm^2$  and mass 1kT.*

### 3 Appearance of Wrong Sign Muons at a NF

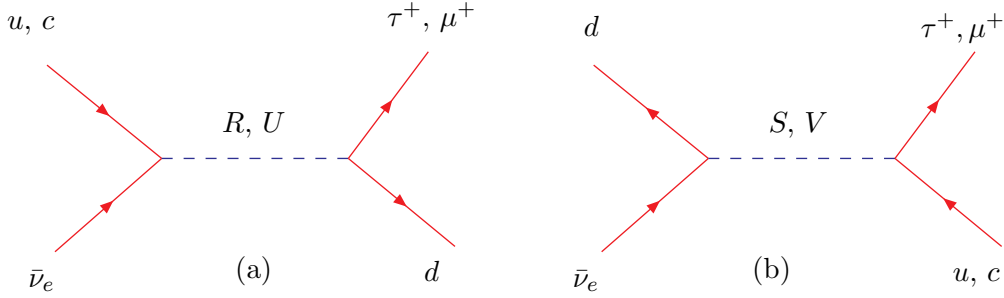


Figure 4: Production of  $\tau^+$  &  $\mu^+$  from scalar & vector LQ: (a) s-channel process corresponding to  $|F| = 0$  LQ and (b) u-channel process corresponding to  $|F| = 2$  LQ.

In the OS,  $\bar{\nu}_e$  from the parent  $\mu^-$  beam can oscillate to either  $\bar{\nu}_\mu$  or to  $\bar{\nu}_\tau$  which give rise to  $\mu^+$  and  $\tau^+$ , respectively. The  $\tau^+$  further decays muonically ( $BR = 17\%$  [14]) and thus contribute to the  $\mu^+$  events. However, it is worthwhile to mention here that one can hardly expect any  $\mu^+$  events from oscillations since the neutrino mass-splitting required for the Mikheyev-Smirnov-Wolfenstein (MSW) solution to the solar neutrino problem [2] with matter-enhanced  $\nu_e$ - $\nu_\mu$  oscillation is  $\Delta m^2 \simeq 10^{-5} eV^2$ . The situation is even worse for the case of Vacuum Oscillation solution which requires  $\Delta m^2 \simeq 10^{-10} eV^2$ . For the  $\nu_e$ - $\nu_\tau$  oscillation, there exists no experimental support and so, the region of parameter space to be explored for such oscillation mode is not known at all. Thus, a significant event rate for wrong sign muons cannot be attributed to  $\nu$ -oscillation effects alone.

Here, we consider the production of  $\mu^+$  from parent  $\mu^-$  beam via *unoscillated*  $\bar{\nu}_e$  through LFV interactions with nucleon mediated by LQ in two different ways: (i) Direct Production of  $\mu^+$  as well as (ii) Production of  $\tau^+$ , which further decays leptonically to  $\mu^+$ . Both of these involve s-channel processes corresponding to  $|F| = 0$  & charge = 2/3 (figure 4(a)) LQ and u-channel processes corresponding to  $|F| = 2$  & charge = -1/3 (figure 4(b)) LQ. In figure 4(a) out of four s-channel diagrams, one is mediated by a scalar LQ ( $R_2^a$ ) with  $T_3 = -1/2$ , while the other three are mediated by vector LQ ( $U_{1\mu}, U_{1\mu}, U_{3\mu}^0$ ) with  $T_3 = 0$  each. The matrix element squared for all the four s-channel processes is

$$\begin{aligned}
 \left| \mathcal{M}_{LQ}^{s-channel}(\bar{\nu}_e u \rightarrow \mu^+ d) \right|^2 &= \left[ \hat{s}(\hat{s} - m_\mu^2) \right] \left[ \frac{|h_{2L} h_{2R}|^2}{(\hat{s} - M_{R_2^a}^2)^2} \right] + \left[ 4(\hat{s} + \hat{t})(\hat{s} + \hat{t} - m_\mu^2) \right] \left[ \frac{|h_{1L}|^4}{(\hat{s} - M_{U_{1\mu}}^2)^2} \right] \\
 &+ \frac{|h_{3L}|^4}{(\hat{s} - M_{U_{3\mu}^0}^2)^2} - 2 \frac{|h_{1L} h_{3L}|^2}{(\hat{s} - M_{U_{1\mu}}^2)(\hat{s} - M_{U_{3\mu}^0}^2)} + \left[ 4\hat{t}(\hat{t} - m_\mu^2) \right] \left[ \frac{|h_{1L} h_{1R}|^2}{(\hat{s} - M_{U_{1\mu}}^2)^2} \right] \quad (5)
 \end{aligned}$$

where,  $\hat{s} = (p_{\bar{\nu}_e} + p_{u,c})^2$ ,  $\hat{t} = (p_{\bar{\nu}_e} - p_{\mu^+})^2$  and  $\hat{u} = (p_{\bar{\nu}_e} - p_d)^2$ , with  $p_i$  denoting the four momentum of the  $i^{th}$  particle. In figure 4(b) out of four u-channel diagrams three are mediated by scalar LQ ( $S_1, S_1, S_3^0$ ) with  $T_3 = 0$  each and the fourth diagram is mediated by a vector LQ ( $V_{2\mu}^a$ ) with  $T_3 = -1/2$ . The matrix element squared for all the four u-channel processes corresponding to  $|F| = 2$  is

$$\left| \mathcal{M}_{LQ}^{u-channel}(\bar{\nu}_e u \rightarrow \mu^+ d) \right|^2 = \left[ \hat{u}(\hat{u} - m_\mu^2) \right] \left[ \frac{|g_{1L}|^4}{(\hat{u} - M_{S_1}^2)^2} + \frac{|g_{1L} g_{1R}|^2}{(\hat{u} - M_{S_1}^2)^2} + \frac{|g_{3L}|^4}{(\hat{u} - M_{S_3^0}^2)^2} \right]$$

$$- 2 \frac{|g_{1L} g_{3L}|^2}{(\hat{u} - M_{S_1}^2)(\hat{u} - M_{S_3}^2)} \Big] + \left[ 4\hat{t}(\hat{t} - m_\mu^2) \right] \left[ \frac{|g_{2L} g_{2R}|^2}{(\hat{u} - M_{V_{2\mu}^a})^2} \right] \quad (6)$$

Similar expressions of matrix element squared for  $s$ - and  $u$ - channel diagrams corresponding

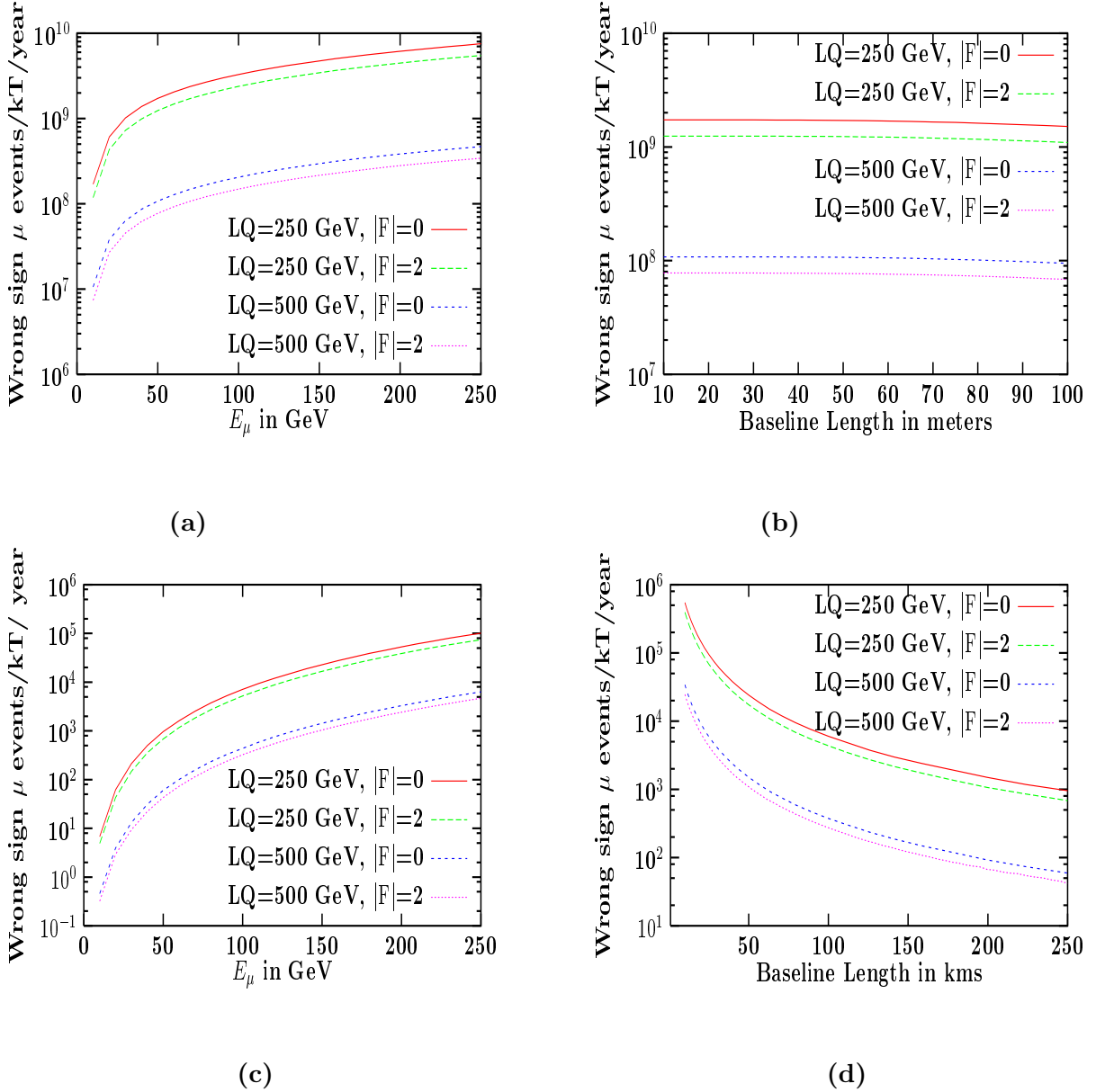


Figure 5: Variation of wrong sign  $\mu$ -events ( from osc. and LQ ) with : (a) muon beam energy for a baseline length 40 meters, (b) baseline length for near-site detector configuration, (c) muon beam energy for a baseline length 250 kms, (d) baseline length for short baseline situation. All the parameters used here are as mentioned in the caption of figure 2.

to the process  $\bar{\nu}_e u \rightarrow \tau^+ d$  can be obtained just by substituting  $m_\mu^2$  by  $m_\tau^2$  and  $p_{\mu^+}$  by  $p_{\tau^+}$  in equations (5) and (6).

In order to study the behaviour of wrong sign muon events w.r.t  $E_\mu$  and baseline length, we have used the same coupling strengths and masses as mentioned in section 2. For the indirect production of  $\mu^+$  via decay of  $\tau^+$  we have taken the efficiency factor for  $\tau$  detection (in leptonic channel) to be 30% [5, 11]. Predictions for wrong sign muon production rate w.r.t  $E_\mu$  and baseline length are plotted in figure 5. The features of the plots for both near-site and

short baseline experiments are same as that for  $\tau$  production case discussed in the previous section.

In our calculation, we have not put any specific selection cut for the production of wrong sign  $\mu$ . However, the muons from charm decay which forms a significant background for the production of wrong sign muons, can be eliminated by incorporating stringent cuts on the transverse momentum of muons, missing  $p_T$  and isolation cut as mentioned in [5, 11, 12].

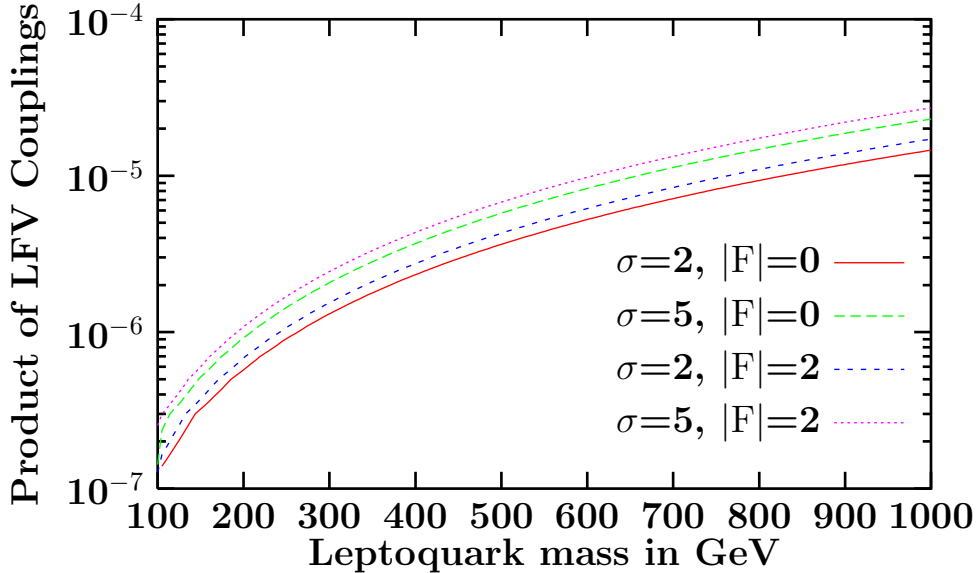


Figure 6: Contour plot for wrong sign muons at  $2\sigma$  and  $5\sigma$  effect for  $E_\mu=50$  GeV, baseline length=40 meters and sample detector of area  $2500$   $\text{cm}^2$  and mass  $1kT$ .

**Sensitivity Limits :** Accepting the requirement of  $2\sigma$  and  $5\sigma$  effect as a sensible discovery criterion, we plot the corresponding contours for the wrong sign muons at a baseline length=40 m in figure 6.

## 4 $\tau$ and Wrong Sign $\mu$ Appearance at a NF and Low Energy Bounds

In sections 2 and 3 for the purpose of illustration, we considered  $|F| = 0$  and  $|F| = 2$  couplings separately and took all couplings to be equal to the electromagnetic coupling,  $\alpha_{em}$ . But as also discussed in the introduction, strong constraints on the LQ couplings and masses have been obtained in the literature from FCNC processes [7]. In particular, bounds obtained from rare  $\tau$  decay  $\tau \rightarrow \pi^0 \mu$  and from  $\mu \leftrightarrow e$  conversion in nuclei would have a direct bearing on the processes considered here. This is because low energy limits put stringent bounds on effective four-fermion interactions involving two leptons and two quarks and since at a NF the centre of mass energy in collisions is low enough, we can consider the neutrino-quark interactions as four-fermion interactions. These bounds on the effective couplings given as LQ couplings over mass squared of the LQ are derived on the assumption that individual LQ coupling contribution to



the branching ratio does not exceed the experimental upper limits and in the branching ratios only one LQ coupling contribution is considered by ‘switching off’ all the other couplings. The couplings are taken to be real but in these studies combinations of left and right chirality couplings are not considered.

Based on these studies, we make some simplified assumptions like obtaining the product of couplings of different chirality from the square of couplings of individual chirality. We extract the coupling products relevant to  $(\nu_\mu d)$   $(\tau u)$  vertex from rare  $\tau$  decay bounds as quoted in the reference [7] and we get the following

$$\begin{aligned}
|h_{1L}|^2 = |h_{1R}|^2 &= 1.9 \times 10^{-3} \left( \frac{M_{LQ}}{100 \text{ GeV}} \right)^2, & |h_{2L}|^2 &= 3.9 \times 10^{-3} \left( \frac{M_{LQ}}{100 \text{ GeV}} \right)^2, \\
|h_{3L}|^2 &= 6.4 \times 10^{-4} \left( \frac{M_{LQ}}{100 \text{ GeV}} \right)^2, & |h_{2R}|^2 &= 1.9 \times 10^{-3} \left( \frac{M_{LQ}}{100 \text{ GeV}} \right)^2, \\
|g_{1L}|^2 = |g_{1R}|^2 &= 3.9 \times 10^{-3} \left( \frac{M_{LQ}}{100 \text{ GeV}} \right)^2, & |g_{3L}|^2 &= 1.3 \times 10^{-3} \left( \frac{M_{LQ}}{100 \text{ GeV}} \right)^2, \\
|g_{2L}|^2 &= 1.9 \times 10^{-3} \left( \frac{M_{LQ}}{100 \text{ GeV}} \right)^2, & |g_{2R}|^2 &= 9.7 \times 10^{-4} \left( \frac{M_{LQ}}{100 \text{ GeV}} \right)^2. \quad (7)
\end{aligned}$$

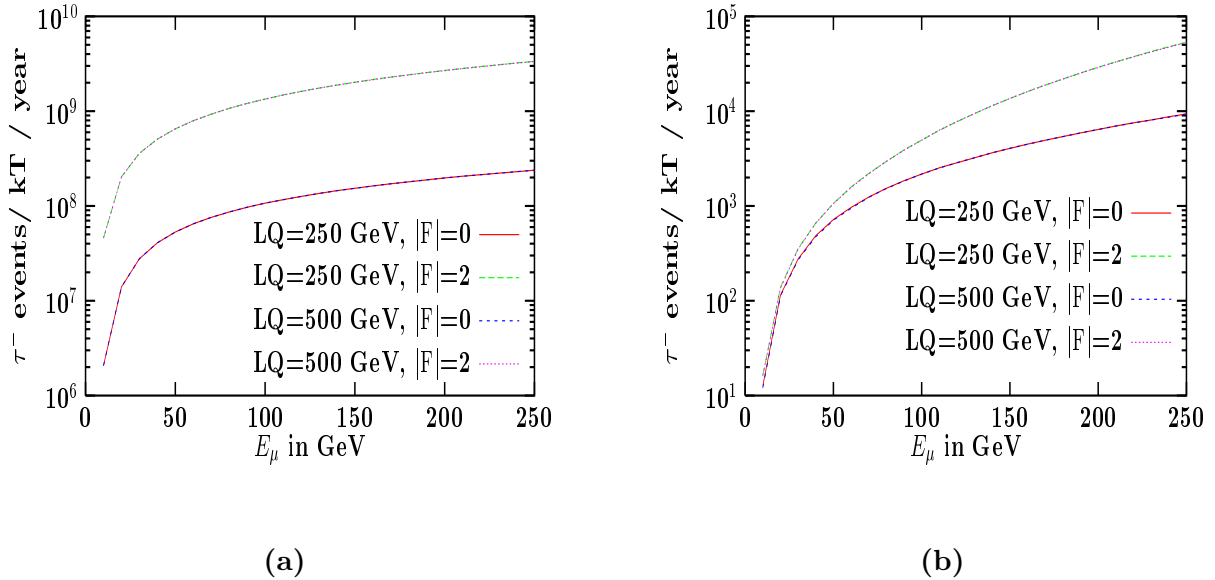


Figure 7: Variation of  $\tau$ -events ( from osc. and LQ ) with : (a) muon beam energy for a baseline length 40 meters, (b) muon beam energy for a baseline length 250 kms. All the parameters used here except for the couplings are as mentioned in the caption of figure 4.

In case of wrong sign  $\mu$ , the bounds on the couplings for  $(\bar{\nu}_e u)(\mu^+ d)$  vertex arising from  $\mu \longleftrightarrow e$  conversion are so stringent, being typically 2-3 orders of magnitude lower compared to bounds on couplings involving third generation of quarks and leptons, that the direct production of  $\mu^+$  is highly suppressed. The relevant coupling constants extracted from [7] are

$$\begin{aligned}
|h_{1L}|^2 = |h_{1R}|^2 &= 2.6 \times 10^{-7} \left( \frac{M_{LQ}}{100 \text{ GeV}} \right)^2, & |h_{2L}|^2 &= 5.2 \times 10^{-7} \left( \frac{M_{LQ}}{100 \text{ GeV}} \right)^2, \\
|h_{3L}|^2 &= 8.5 \times 10^{-8} \left( \frac{M_{LQ}}{100 \text{ GeV}} \right)^2, & |h_{2R}|^2 &= 2.6 \times 10^{-7} \left( \frac{M_{LQ}}{100 \text{ GeV}} \right)^2, \\
|g_{1L}|^2 = |g_{1R}|^2 &= 5.2 \times 10^{-7} \left( \frac{M_{LQ}}{100 \text{ GeV}} \right)^2, & |g_{3L}|^2 &= 1.7 \times 10^{-7} \left( \frac{M_{LQ}}{100 \text{ GeV}} \right)^2,
\end{aligned}$$

$$|g_{2L}|^2 = 2.6 \times 10^{-7} \left( \frac{M_{LQ}}{100 \text{ GeV}} \right)^2, \quad |g_{2R}|^2 = 1.3 \times 10^{-7} \left( \frac{M_{LQ}}{100 \text{ GeV}} \right)^2. \quad (8)$$

In this situation, wrong sign muons mainly arise through the production of  $\tau^+$ 's, which subsequently decay via leptonic channel. The bounds on coupling constants for the  $(\bar{\nu}_e u)(\tau^+ d)$  vertex come from the decay  $\tau \rightarrow \pi^0 e$  and are essentially the same as that for the case of  $\tau$  production [7].

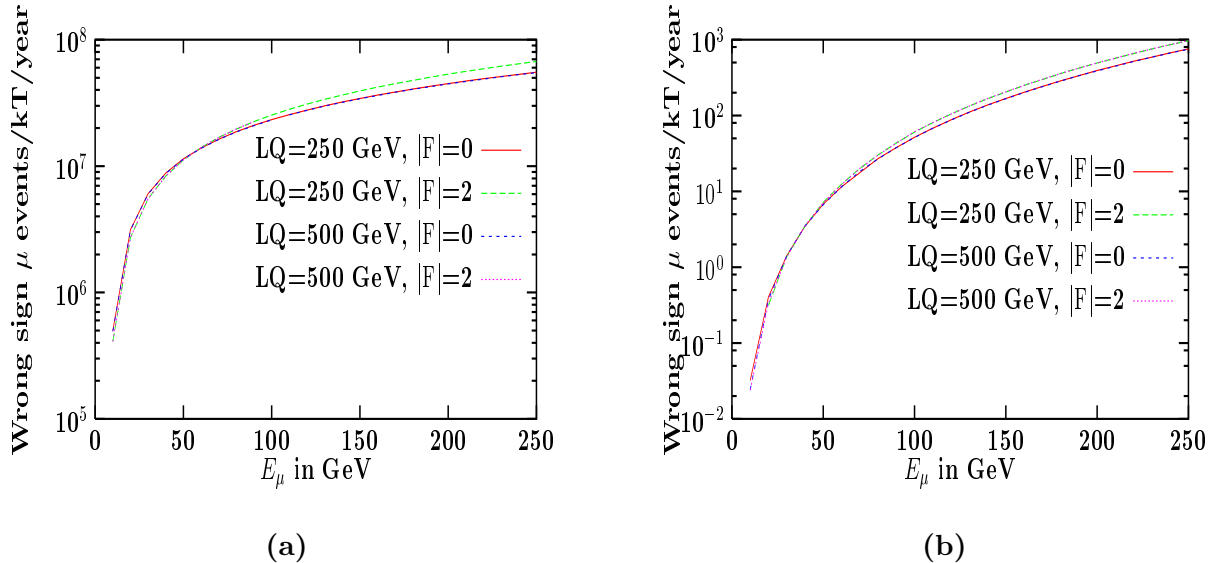


Figure 8: Variation of wrong sign  $\mu$ -events ( from osc. and LQ ) with : (a) muon beam energy for a baseline length 40 meters, (b) muon beam energy for a baseline length 250 kms. All parameters used here for plotting except for couplings are as quoted in the caption of figure 5.

In figure 7 we show the variation of  $\tau$  events with muon beam energy and in figure 8, the variation of wrong sign muons with muon energy for the baseline lengths of 40 m and 250 km respectively. The graphs clearly show that number of  $\tau$ / wrong sign muons are independent of LQ masses, as expected. On comparing figures 7 & 8 with figures 2 & 5 respectively, we find considerable suppression in event rates.

We should however bear in mind that rare decay bounds in LQ interactions with a charm quark are comparatively weak and therefore these bounds can be evaded if we can tag the charm production.

## 5 Conclusions

NF will open up unprecedented opportunities to investigate  $\nu$  physics, bearing not only on  $\nu$  oscillation phenomenon but also providing physical laboratory for testing physics beyond the SM. In this letter, we investigated the LFV effect in theories with LQ on the production of  $\tau$ 's and wrong sign  $\mu$ 's in the near and short baseline experiments. It is clear that with the increase in baseline length, the LQ event rate falls off and neutrino oscillations are the main source events examined here. At near-site experiments, on the other hand, the events mainly arise from *new interactions* and can thus be used to constrain the theory (figures 3-8). In particular one can obtain constraints on LFV couplings between the first and third generation, the bounds on which are generally not available. At near-site experiments, the event rate is practically independent of baseline length.

**Acknowledgment:** We are grateful to Namit Mahajan, Debajyoti Choudhury and Anindya Datta for useful discussions. P.M. acknowledges Council for Scientific and Industrial Research, India while A.G. acknowledges the University Grants Commission, India for partial financial support.

## References

- [1] Y. Suzuki, H. Sobel, T. Mann and B. Barish; Talks given at the XIX International Conference on Neutrino Physics & Astrophysics, see, <http://nu2000.sno.laurentian.ca/>; S. Rigolin, (hep-ph/0002108).
- [2] J. J. Bahcall, P. I. Krastev, A. Yu. Smirnov, Phys. Rev. **D58**, 096016 (1998); Phys. Rev. **D60**, 093991 (1999); (hep-ex/0103179); M. Gozalez-Garcia, Talk given at the XIX International Conference on Neutrino Physics & Astrophysics, see,[http://nu2000.sno.laurentian.ca/M. Gonzalez-Garcia](http://nu2000.sno.laurentian.ca/M.Gonzalez-Garcia).
- [3] C. Quigg, (hep-ph/9803326); S. Geer, Phys. Rev. **D57**, 6989 (1998); D. Ayres *et al.*, (electronic archive: physics/9911009); A. Cervera *et al.*,(hep-ph/0002108); A. Blondel *et al.*, CERN-EP-2000-05; C. Albright *et al.*, (hep-ex/0008064); S. Geer, (hep-ph/0008155); M. L. Mangano *et al.*, (hep-ph/0105155), CERN-TH/2001-131.
- [4] A. De Rujula, M.B. Gavela, P. Hernandez, Nucl. Phys. **B547**, 21 (1999); S. Dutta, R. Gandhi, B. Mukhopadhyaya, Euro. Phys. J.**C18**, 405 (2000); V. Barger, S. Geer, R. Raja, K. Whisnant, Phys. Lett. **B485**, 379 (2000); Phys. Rev. **D62**, 013004 (2000); I. Mocioiu and Robert Shrock, Phys. Rev. **D62**, 053017 (2000).
- [5] A. Datta, R. Gandhi, B. Mukhopadhyaya, P. Mehta, Phys. Rev. **D64**, 015011 (2001); D. Chakraverty, A. Datta, B. Mukhopadhyaya, Phys. Lett. **B503**, 74 (2001).
- [6] J. C. Pati and Abdus Salam, Phys. Rev. **D10**, 275 (1974); O. Shankar, Nucl. Phys. **B206**, 253 (1982); W. Buchmuller and D. Wyler, Phys. Lett. **B177**, 377 (1986); W. Buchmuller, R. Ruckl, D. Wyler, Phys. Lett. **B191**, 442 (1987); P. Langacker, M. Luo, Alfred K Mann, Rev. Mod. Phys. **64**, 87 (1992); J. Blumlein and R. Ruckl, Phys. Lett. **B304**, 337 (1993); M. A. Doncheski and R. W. Robinett, Phys. Rev. **D56**, 7412 (1997); U. Mahanta, Phys. Rev. **D62**, 073009 (2000).
- [7] S. Davidson, D. Bailey, B. A. Campbell, Z. Phys. **C61**, 613 (1994); E. Gabrielli, Phys. Rev. **D62**, 055009 (2000).
- [8] S. Aid *et al.* Phys. Lett. **B353**, 578 (1995); Derrick *et al.*, Z. Phys. **C73**, 613 (1997); C. Adloff *et al.*, (hep-ex/9907002).
- [9] See the third and sixth references in [6].
- [10] H. Lai *et al.*, Phys. Rev. **D55**, 1280 (1997).
- [11] C. Albright *et al.*, (hep-ex/0008064).
- [12] See the second reference in [4] and references therein.
- [13] P. Migliozi *et al.*, (hep-ph/0011051).
- [14] Particle Data Group, D. E. Groom *et al.*, The European Phys. Jr. **C15**, 1 (2000).